

Lightweight Contrastive Protein Structure-Sequence Transformation

Jiangbin Zheng^{1,2}, Ge Wang^{1,2}, Bozhen Hu^{1,2}, Yufei Huang^{1,2},
Siyuan Li^{1,2}, Cheng Tan^{1,2}, Xinwen Fan^{3,4}, Stan Z. Li^{2,*}

¹Zhejiang University

²AI Division, School of Engineering, Westlake University

³School of Life Sciences, Westlake University

⁴Institute of Basic Medical Sciences, Westlake Institute for Advanced Study

{zhengjiangbin, wangge, hubozhen, huangyufei, lisiyuan,
tancheng, fanxinwen, Stan.ZQ.Li}@westlake.edu.cn

Abstract

Pretrained protein structure models without labels are crucial foundations for the majority of protein downstream applications. The conventional structure pretraining methods follow the mature natural language pretraining methods such as denoised reconstruction and masked language modeling but usually destroy the real representation of spatial structures. The other common pretraining methods might predict a fixed set of predetermined object categories, where a restricted supervised manner limits their generality and usability as additional labeled data is required to specify any other protein concepts. In this work, we introduce a novel unsupervised protein structure representation pretraining with a robust protein language model. In particular, we first propose to leverage an existing pretrained language model to guide structure model learning through an unsupervised contrastive alignment. In addition, a self-supervised structure constraint is proposed to further learn the intrinsic information about the structures. With only light training data, the pretrained structure model can obtain better generalization ability. To quantitatively evaluate the proposed structure models, we design a series of rational evaluation methods, including internal tasks (e.g., contact map prediction, distribution alignment quality) and external/downstream tasks (e.g., protein design). The extensive experimental results conducted on multiple tasks and specific datasets demonstrate the superiority of the proposed sequence-structure transformation framework.

1. Introduction

Deep learning has witnessed the power of protein-related fields, especially for the protein structure prediction task (represented by AlphaFold2 [22]) and protein design task

(represented by ESM-IF [16], ProteinMPNN [16]). The target of protein structure prediction is to generate the 3D structures from the corresponding protein sequences (i.e., amino acid sequences), while the protein design is an almost inverted task.

Generally, deep protein tasks involve protein sequence and protein structure. Thus protein language model and protein structure model become the most two fundamental components for downstream tasks. For the protein language modeling, there are a variety of available models [5, 26, 32, 33, 35] due to mature pretraining techniques and more simple textual representation [38, 41, 44]. Among them, denoised reconstruction and masked language modeling (MLM) based protein language models [9] have become the most commonly-used pretraining modes. However, there are few universal pretrained protein structure models. Since the complex and continuous spatial structures of proteins, applying similar operations of protein language model pretraining such as adding noise and masking coordinate sequences for structure model pretraining might damage the original real structural space and even result in radically different semantic representation. Therefore, the existing most effective structure models are almost task-specific in a supervised manner and not suitable for large-scale unsupervised pretraining.

Rethinking the current advanced protein structure prediction models (i.e., sequence-to-structure models) which reach even atom-level high-accuracy transformation performances approaching the experimental level, this observation clearly indicates that protein sequence representations naturally contain abundant structural information. Therefore, *is it possible to enhance the training of protein structure models guided by reliable and robust pretrained protein language models?* Fortunately, emerging pretraining methods in the typical text-image cross-modal domain rep-

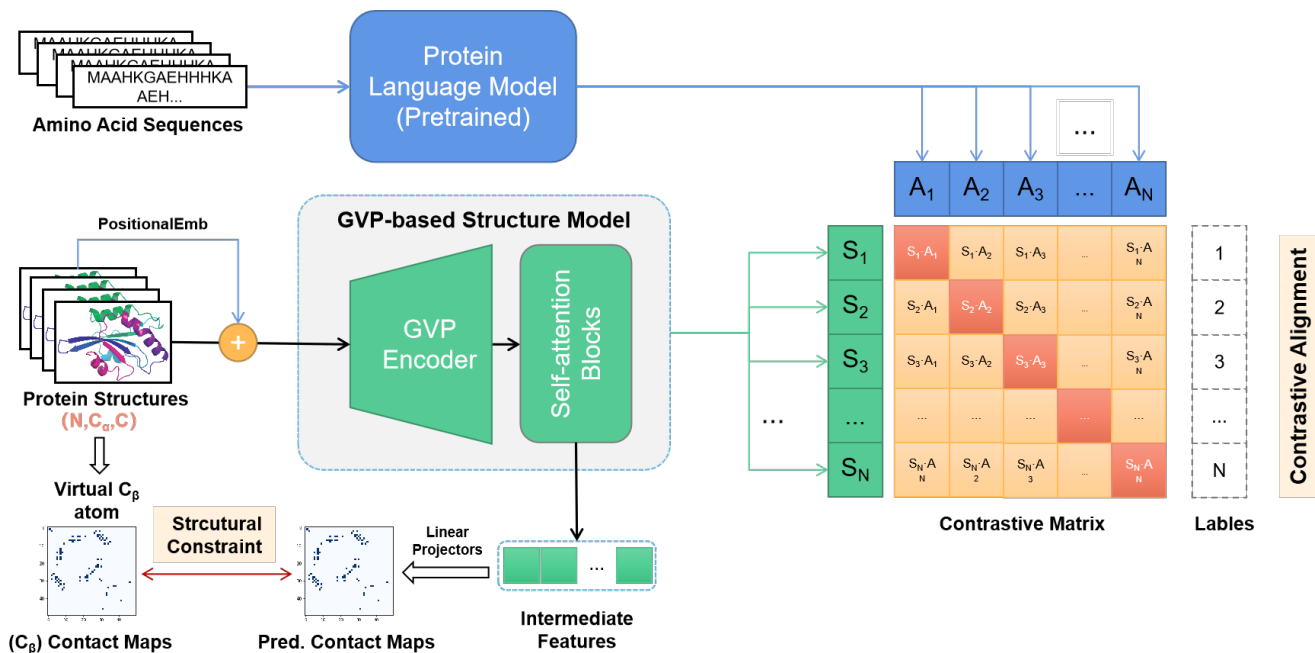


Figure 1. The proposed sequence-structure transformation framework. We use a pretrained protein language model to guide the training of the protein structure model with contrast alignment loss. To facilitate internal evaluation and to strengthen the information constraints on the structure, we propose to predict contact maps based on C_β as a self-supervised loss, where virtual C_β atoms can be computed from three atoms of N, C_α , and O.

represented by CLIP [29, 30] bring us direct inspiration, where large-scale textual pretrained language models are used to pretrain visual models for intermediate feature alignment. The success of CLIP thus also implies that we can treat protein structure and sequence as two different modalities and then adopt a similar cross-modal alignment pretraining strategy, which makes the existing large-scale protein language modalities potential to be used for training protein structure modalities.

In this work, we propose a novel contrastive protein sequence-structure transformation for protein structure model pretraining. Specifically, we utilize an unsupervised contrastive alignment between the protein sequence representation and protein structure representation. To pretrain the model, random structure-sequence parallel pairs are selected for building mini-batches, which not only establish the cross-modal alignment relationships but also obtain negative samples from other pairs naturally for contrastive learning. Furthermore, to strengthen the constraint of structural representation, we propose a self-supervised contact map constraint based on intermediate features from the structure encoder.

To evaluate the proposed sequence-structure transformation framework, quantitative and qualitative experiments should be conducted. However, as a brand-new protein pretraining paradigm, there are no complete reference evaluation strategies. Hence, we additionally introduce a series

of evaluation experiments to comprehensively prove the robustness of our trained structure model. In particular, internal tasks (e.g., contact map prediction evaluation, and distribution alignment quality evaluation) are proposed to show the internal contrastive alignment ability and distillation performances, while external/downstream tasks (e.g., protein design task) are proposed to show the generalization ability of pretrained protein structure model. In the proposed evaluation system, the sequence-structure transformation framework is experimentally validated, which fully shows the robustness of the pretraining performance. For example, the downstream protein design task achieves excellent performance on lower perplexity and higher sequence recovery.

The contributions are summarized as follows:

- The proposed unsupervised protein sequence-structure transformation framework establishes a novel deep alignment relationship between protein sequences and protein structures.
- Based on the proposed contrastive transformation framework, we first pretrain the protein structure model under the guidance of abundant prior language knowledge from the pretrained protein sequence model.
- To evaluate the pretrained structure model, we propose

a complete evaluation system, where evaluation metrics and evaluation tasks including internal and downstream tasks are introduced, providing baselines for the protein structure research community.

- The proposed protein structure model pretraining achieves competitive performances among various evaluation tasks, such as a superior performance in the protein design task.

2. Related Work

Protein Language Models. Inspired by recent breakthroughs in natural language processing and similarities between human languages and protein sequences, protein language modeling has emerged as an active and promising direction for unsupervised learning of protein primary structures [1, 2, 17, 18, 42]. UniRep [1], UDSMProt [36] and SeqVec [14] use LSTM or its variants to learn sequence representations and long-range dependencies. TAPE [31] benchmarks a group of protein models through various tasks, concluding the effectiveness of the self-supervised pretraining methods. Much work has improved the model scale and architecture to learn more protein semantics. Elnaggar et al. [10] have trained several successful transformer variants on billions of amino acid sequences. Similarly, ESM-1b [34] employs a Transformer architecture and a masked language modelling strategy to train robust representations based on a large-scale dataset. And ESM-2 [25] then extends ESM-1b with larger-scale parameters (15 billion), which achieves more superior results compared with other smaller ESM models.

Protein Structure Models. As the function of a protein is usually determined by its structure, structure-based protein models are also the crucial solution for learning a representative protein embedding. Thanks to the advances in highly accurate deep learning-based protein structure prediction methods [3, 23], AlphaFoldDB [39] has provided over 200 million protein structure predictions to accelerate scientific research. Based on this development, more and more protein structure models have appeared, which commonly seek to encode the spatial information of protein structures by convolutional neural networks (CNNs) [8] or graph neural networks (GNNs) [4, 12, 21]. Among these methods, SPROF [6] employs distance maps to predict protein sequence profiles. And IEConv [15] introduces a convolution operator to capture all relevant structural levels of a protein. GearNet [43] encodes the spatial information by adding different types of sequential or structural edges and then performed relational message passing on protein residue graphs. GVP-GNN [21] designed the geometric vector perceptrons (GVP) to learn both scalar and vector features in an equivariant and invariant manner, while Guo et al. [13] adopted SE(3)-invariant features as the model

inputs and reconstructed gradients over 3D coordinates to avoid the usage of complicated SE(3)-equivariant models.

3. Methods

In this section, we describe the proposed sequence-structure transformation framework in detail. As shown in Figure 1, to train the protein structure model, a pretrained protein language model is used as the teacher model to guide the pretraining of the protein structure model. The contrastive alignment constraint learns prior pretrained language information, and the internal contact map reconstruction task assists structure learning in an unsupervised manner.

3.1. Pretrained Sequence Module

Pretrained protein sequence/language models have been widely used in deep protein downstream tasks, which are typically trained on large-scale datasets. Since sequence models implicitly include abundant structural information learned from existing sequence data, a robust protein language model can serve as a teacher to guide the structure model learning. We adopt the ESM-2 [26] as the primary teacher among the existing language models. Note that in this work ESM-2 base is utilized since this version has fewer parameters without a significant loss of precision.

The ESM-2 language model is a high-performance protein language model. Compared to previous generation models such as ESM-1b [32], ESM-2 has improved model architecture, training techniques, and increased computational resources and data. The addition of relative positional embeddings in ESM-2 makes generalization to arbitrary length sequences possible. These modifications resulted in a significantly better model.

3.2. Equivariant Structure Module

For downstream protein structure tasks such as inverse folding, the predicted sequence should be independent of the reference frame of the structural coordinates. In other words, for any rotation and translation \mathcal{F} of the input coordinates X , the output distribution Y of the model is expected to be invariant under these transformations, i.e., $p(Y|X) = p(Y|\mathcal{F}(X))$. To satisfy this condition, equivariant network models are widely used in protein 3D structure modeling, where geometric vector perceptron (GVP)-based models such as GVP-GNN [20] and GVP-Transformer [16] have achieved impressive performance in protein design tasks. This suggests that the GVP module plays an important role in representing structural features to maintain equivariant properties. Furthermore, the GVP components are simple and lightweight, thus the GVP architecture is adapted as the structure module, as shown in Figure 2.

We first use the GVP-GNN encoder layers to extract spatial geometric features, and then a generic Transformer

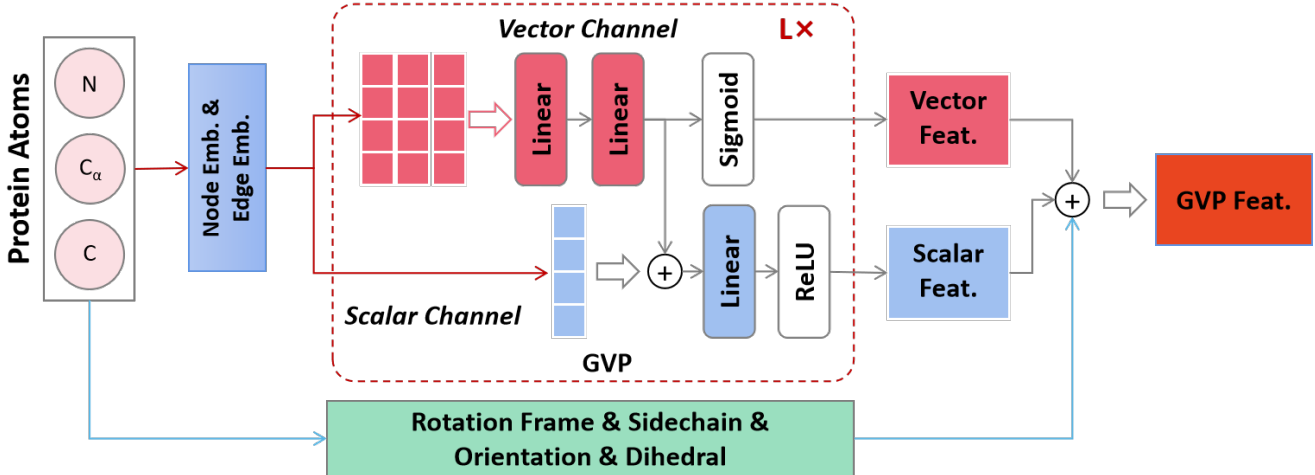


Figure 2. Schematic diagram of the GVP module. Protein backbone atoms (C, C_α and N) are used to generate graphs with node and edge features based on k-nearest neighbor relationships. The graphs are fed into the vector channel and scalar channel of the GVP module to generate vector and scalar features, respectively. These two primary features are then combined with additional spatial features such as rotation frame, sidechain, orientation, and dihedral features to form the spatial structure features.

based self-attention blocks [40] to extract temporal features. In GVP-GNN, the input features are translation-invariant and each layer is rotation-equivariant. We perform a change of basis on the vector features from GVP-GNN into local reference frames defined for each amino acid to derive rotation-invariant features [16]. Besides, different from the generic Transformer, the learned positional embeddings are used instead of sinusoidal positional embeddings.

3.3. Cross-modal Pretraining Objectives

3.3.1 Contrastive Alignment Loss

Aligning both structural and textual modalities can improve multi-modality framework [27]. To enforce cross-modality alignment constraints, we propose a contrastive alignment loss for protein language and structure models.

Previous cross-modality alignment mostly focuses on positive samples only [45]. Inspired by contrastive learning [46], we construct both positive and negative samples in the same mini-batch and implement a contrastive cross-modal alignment method to ensure that similar features are closer while different features are farther apart. Given that the normalized structural features from GVP as $\mathcal{S}_{\text{logits}} \in \mathbb{R}^{B \times T \times d}$, and the normalized temporal features from self-attention layers as $\mathcal{V}_{\text{logits}} \in \mathbb{R}^{B \times T \times d}$, where B is the number of samples, T is the maximum length of sequences and d is the dimension of features. Then the pair matrices are computed firstly as:

$$\mathcal{S2V}_{\text{pair}} = \mathcal{S}_{\text{logits}} \times \mathcal{V}_{\text{logits}}^T, \quad (1)$$

$$\mathcal{V2S}_{\text{pair}} = \mathcal{V}_{\text{logits}} \times \mathcal{S}_{\text{logits}}^T, \quad (2)$$

Taking $\mathcal{S2V}_{\text{pair}} \in \mathbb{R}^{B \times B}$ pair matrix (denoted as \mathcal{P}) as an example, $\mathcal{P}[i, j] (0 \leq i, j < B)$ represents the similar-

ity value between the structural feature of the i -th batch and the textual feature of j -th batch. The structural and textual features from the same input instances are positive samples, and the features from other different input instances are negative samples. Hence, in the matrix \mathcal{P} , the diagonal similarity values are from positive sample pairs, and the rest values are from negative sample pairs. To make the loss computation differentiable and easy, we convert the computation of positive and negative pairs into a binary classification task [29]. The value i corresponding to the i -th row in the matrix \mathcal{P} is a positive label. Therefore, the corresponding labels of \mathcal{P} are Labels = $\{0, 1, \dots, i, \dots, B\}$, then the contrastive alignment loss related to $\mathcal{S2V}_{\text{pair}}$ as:

$$\mathcal{L}_{\text{align}_s} = \text{CrossEntropy}(\text{Softmax}(\mathcal{S2V}_{\text{pair}}), \text{Labels}). \quad (3)$$

Similarly, the temporal-to-spatial alignment loss related to $\mathcal{V2S}_{\text{pair}}$ as:

$$\mathcal{L}_{\text{align}_v} = \text{CrossEntropy}(\text{Softmax}(\mathcal{V2S}_{\text{pair}}), \text{Labels}). \quad (4)$$

Therefore, the complete contrastive alignment loss as:

$$\mathcal{L}_{\text{align}} = \frac{1}{2}(\mathcal{L}_{\text{align}_s} + \mathcal{L}_{\text{align}_v}). \quad (5)$$

3.3.2 Contrastive Alignment Level

As shown in Figure 3, we propose to compute the alignment loss at the residue level and protein level, respectively. For residue-level alignment, we compare the encoded sequence and structure features residue by residue. While for protein-level alignment, we compare the encoded features at a coarser fine-grained level. Intuitively, alignment

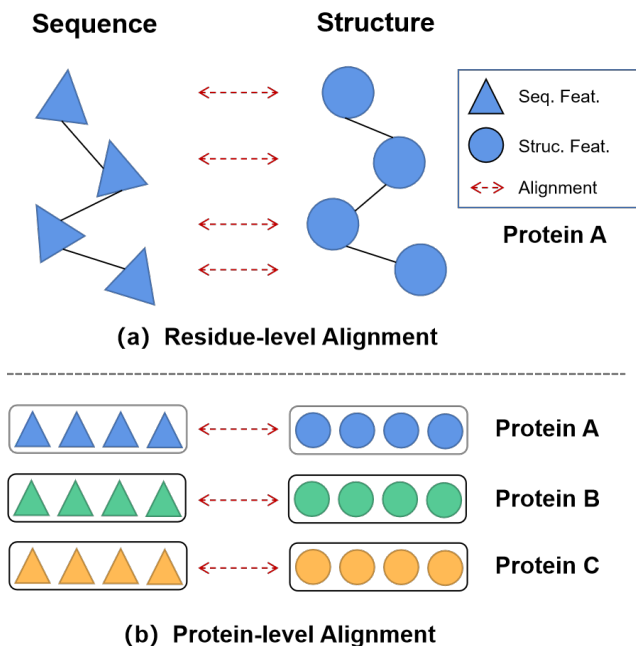


Figure 3. Schematic diagram of different alignment levels. (a) Residue-level alignment is the comparison of each pair of structure-sequence features residue by residue. (b) Protein-level alignment is the comparison of each pair of structure-sequence features protein by protein, where the features of each protein are combined from all the residue features contained in that protein. The same colors indicate a sequence-structure pair from the same protein.

at different fine-grained levels leads to different capabilities. Finer-grained comparisons such as residue-level alignment require more complex computations, but may have better performance. Coarse-grained comparison alignments such as protein-level alignment may perform worse, but are an option worth considering due to their lighter computation. See our experimental section for a detailed analysis. It is worth mentioning that no matter which level is used for calculation, the samples in the mini-batch will be randomly disrupted, and each pairing is different, which is also an implicit data augmentation.

3.4. Structural Reconstruction Loss

As mentioned above, the GVP layers encode N, C_α and O atoms as the core structural feature representation. To strengthen the structural constraints, we propose a self-supervised structure reconstruction task. For constructing a self-supervised structural reconstruction method, predicting the coordinates of virtual C_β atom given the structural features of N, C_α and O atoms is the most direct way, but in practice, it is difficult to predict the coordinates accurately. Therefore, we simplify the difficulty by converting the coordinate prediction to a contact map prediction, as

shown in Figure 4. Specifically, we take the intermediate features (i.e., attention maps) provided by the self-attention blocks shown in Figure 2 to predict the C_β related contact maps [32]. In addition to the constraint of structural information during training, the introduction of a contact map generation can be also used as a metric for the internal performance evaluation of the pretrained model.

Virtual C_β Atom. The C_β is a virtual coordinate that might not appear real in every residue. But by calculating the spatial relationship between N, C_α , and O in the protein backbone, we can obtain the position of the virtual C_β atom as a reference coordinate, calculated as:

$$\begin{aligned}
 D_0 &= P_{C_\alpha} - P_N, \\
 D_1 &= P_C - P_{C_\alpha}, \\
 D_2 &= D_0 \otimes D_1, \\
 P_{C_\beta} &= C_0 \times D_0 + C_1 \times D_1 + C_2 \times D_2 + P_{C_\alpha},
 \end{aligned} \tag{6}$$

where \otimes denotes the cross product of vectors and $P_{(*)}$ denotes the coordinates of the corresponding atom. And $C_0 = 0.56802827$, $C_1 = -0.54067466$ and $C_2 = -0.58273431$ are constant coefficients.

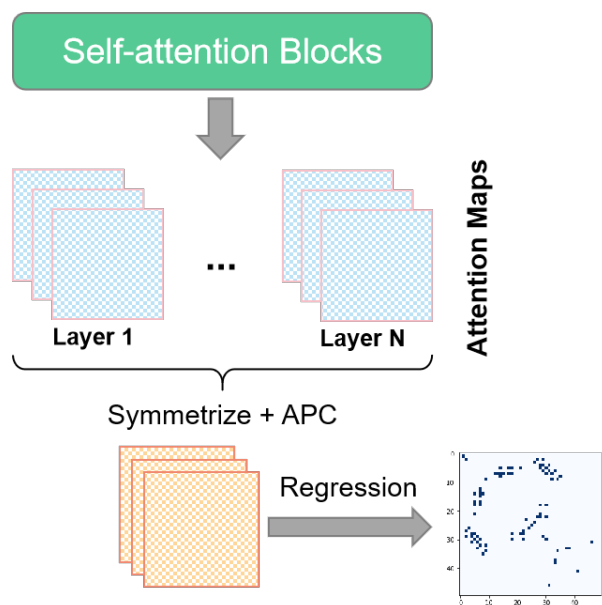


Figure 4. Pipeline of contact map reconstruction based on C_β atoms with length L . Attention maps are extracted from each layer of the self-attention blocks, and then an $L \times L$ coupling matrix is generated by a symmetrization operation and average product correction (APC) along the amino acid dimensions. Then a regression layer is applied to this coupling matrix to determine the final contact map predictions.

Contact Map Predictor. As shown in Figure 4, we show the pipeline diagram of the contact map predictor. The self-attention maps extracted from the self-attention blocks

Group	Level	CATH Test Set			trRosetta Set			TS500 Set			Ts50 Set			CASP14 Set		
		P@L	P@L2	P@L5	P@L	P@L2	P@L5	P@L	P@L2	P@L5	P@L	P@L2	P@L5	P@L	P@L2	P@L5
1	residue	78.05	90.97	96.12	87.69	94.94	96.89	90.31	96.67	98.10	91.36	98.66	100.00	74.9	91.49	95.34
	protein	72.21	88.03	98.31	81.30	92.42	96.18	83.78	94.14	97.44	85.18	96.32	99.53	68.24	87.23	93.96
		acc ₁	acc ₂	KL	acc ₁	acc ₂	KL	acc ₁	acc ₂	KL	acc ₁	acc ₂	KL	acc ₁	acc ₂	KL
2	residue	87.71	87.65	0.004	96.13	96.23	0.0001	94.69	95.02	0.0001	98.29	98.41	0.0001	30.87	30.45	0.0001
	protein	100.00	100.00	0.00	100.00	100.00	0.00	100.00	100.00	0.00	100.00	100.00	0.00	100.00	100.00	0.00

Table 1. Internal evaluation on different test sets. Group 1 shows the performance of contact map predictions on P@L, P@L2 and P@L5 scores with the residue-level and protein-level pretrained models, respectively. Group 2 shows the performance of retrieval alignment evaluations on alignment accuracy and KL distance with residue-level and protein-level pretrained models, respectively. The acc₁ and acc₂ respectively represent the accuracy of structure-to-sequence and sequence-to-structure alignment scores in the contrastive algorithm.

are symmetrized and average product corrected to obtain the final contact maps. The target of the self-supervised structural loss aims to constrain the structural feature representation, and the loss is calculated based on the cross-entropy as:

$$\mathcal{L}_{contact} = \text{CrossEntropy}(M_{ref}, M_{pred}), \quad (7)$$

where M_{ref} denotes the ground-truth contact maps and M_{pred} denotes the predicted contact maps.

Overall, the objective of pretraining is jointly optimized contrastive alignment loss \mathcal{L}_{align} , and contact map loss $\mathcal{L}_{contact}$ as:

$$\mathcal{L}_{pretrain} = \lambda_1 \times \mathcal{L}_{align} + \lambda_2 \times \mathcal{L}_{contact}, \quad (8)$$

where λ_1 and λ_2 are the weighted values.

4. Experiments

4.1. Settings

4.1.1 Evaluation Tasks

Evaluating pretrained protein structure model is intractable, especially for a brand new training framework. Therefore, we build a new evaluation system with multiple internal and external/downstream tasks to demonstrate the learned representation ability, alignment ability, downstream generalization ability, etc.

Internal Evaluation. For internal tasks, we introduce a contact map prediction task and a self-similarity evaluation task. 1) The contact map prediction task uses the top-L long-range precision (P@L) metric to evaluate the quality of the generated contact maps. 2) The self-similarity alignment tasks uses the accuracy and KL divergence metrics to reflect the alignment ability between the language model and the structure model.

External Evaluation. External tasks refer to downstream tasks specifically here. We introduce the protein sequence design task (also known as protein inverse folding), which predicts the corresponding protein sequences given the protein backbone atomic coordinates. The mostly used

metrics for protein design is perplexity and accuracy of recovery.

4.1.2 Datasets

Pretraining Dataset. We leverage a larger-scale protein dataset PDB70 with corresponding protein sequence-structure pairs as the pretraining dataset. To prevent label leakage, we remove all existing data that also appear in evaluation datasets.

Evaluation Datasets. CATH 4.2 dataset [19] is widely used in protein-related work, and its training, validation, and test splits consist of 18204, 608, and 1120 protein data, respectively. In downstream protein design tasks, the training set of CATH is used to fine-tune the pretrained structure model, and the test set of CATH is used for evaluation. We also report results on TS50 & TS500 [24], where Ts50 contains only 50 instances and Ts500 contains 500 instances. Besides, the trRosetta set is often used for contact map prediction tasks. It includes about 15k instances, each of which includes structure, sequence, MSAs and etc. The CASP14 set is known as AlphaFold2 [22]. Although CASP14 is small in number, it is closer to the practice environment of blind tests and competitions. The full CASP14 targets can be found in Appendix Section 5. In short, the trRosetta set, CATH testing set, Ts50/Ts500, and CASP14 set are all used for internal evaluation.

4.1.3 Implementation Details

During pre-training, our structure-to-sequence transformation network is pretrained using the AdamW optimizer with a batch size of 8 and an initial learning rate of 1e-3. The teacher protein language model we use defaults to the ESM-2 base version, and we fix the parameters in the training pipeline. GVP module is set to 4 layers. 0.1 dropout, top-k neighbors 30, node hidden dimension of scalar features 1024, node hidden dimension of vector features 256. And the self-attention block that follow the GVP includes 4 self-attention layers, 8 attention heads, embedded dimension 512, and an attention dropout of 0.1. Note that we

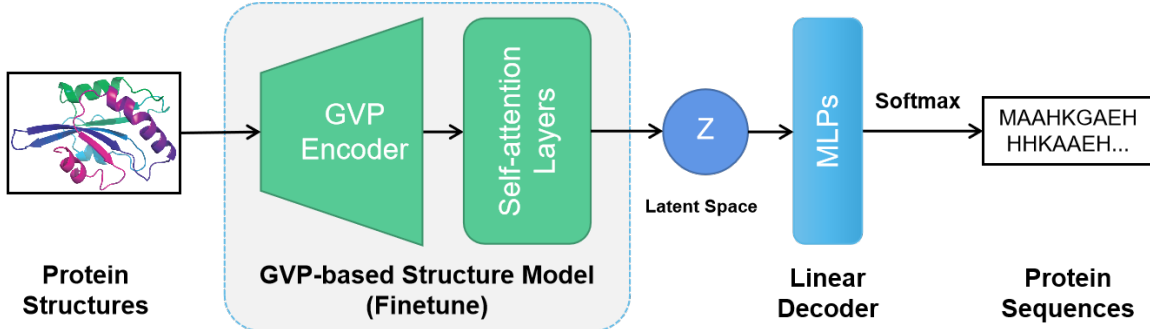


Figure 5. Illustration of the protein design model. We use a GVP-based structure model as an encoder, which captures protein structure features in a latent space. The latent features are then fed into the MLP layers to decode and generate protein sequences. The pretrained structure module is finetuned in the protein design task.

Group	Models	Perplexity			Recovery (%)		
		CATH	Ts50	Ts500	CATH	Ts50	Ts500
1	*Natural frequencies [16]	17.97	-	-	9.5	-	-
	SPIN [24]	-	-	-	-	30.3	30.3
	SPIN2 [28]	-	-	-	-	33.6	36.6
	Structured Transformer [19]	6.85	5.60	5.16	36.4	42.40	44.66
	Structured GNN [20]	6.55	5.40	4.98	37.3	43.89	45.69
	*GVP-Transformer [16]	6.44	-	-	38.3	-	-
	AlphaDesign [11]	6.30	5.25	4.93	41.31	48.36	49.23
	*GVP-GNN-large [20]	6.17	-	-	39.2	-	-
	GCV [37]	6.05	5.09	4.72	37.64	47.02	47.74
	GVP-GNN [20]	5.29	4.71	4.20	40.2	44.14	49.14
	ProteinMPNN [7]	4.61	3.93	3.53	45.96	54.43	58.08
2	Design _r (w/ Pretraining)	4.48	3.76	3.28	50.8	55.8	60.3
	Design _p (w/ Pretraining)	<u>4.51</u>	<u>3.82</u>	<u>3.35</u>	<u>50.1</u>	<u>55.7</u>	<u>59.5</u>
	Design (w/o Pretraining)	6.27	5.05	4.87	39.62	49.21	50.01

Table 2. Comparison of perplexity and recovery among the proposed protein design model (Group 2) and other baselines (Group 1) on the CATH, Ts50 and Ts500 datasets. The best result is **bolded**, followed by underlined. All models here are trained/finetuned on the CATH training set. Design_p: protein-level pretrained model; Design_r: residue-level pretrained model; *: evaluated on the CATH 4.3 test set; Others: evaluated on the CATH 4.2 test set. (Note: Most of the experiments were evaluated on the CATH 4.2 dataset, but part of the work used CATH 4.3 due to version issues. The distribution of data sampled by the two versions is similar, so the trends and conclusions of the results are similar.)

pretrain the model for residue-level alignment and protein-level alignment independently.

4.2. Internal Evaluation

Contact Map Prediction. Contact map predictions reflect the structural representation capabilities. Since we use the gradient backpropagation mechanism in the pretraining stage, the contact map predictor can generate contact maps directly without finetuning. The contact map prediction scores are shown in Group 1 of Table 1, which are evaluated on CATH, trRosetta, Ts50/Ts500 and CASP14 test sets. Both the residue-level and protein-level pretrained models achieve high P@L accuracy in predicting contact maps for

all datasets, implying that the pretrained structure module has learned rich structural representations. Within Group 1, the residue-level evaluation has better performance, probably due to its fine-graininess.

Retrieval Alignment Evaluation. In the proposed pretraining framework, a strong assumption is that protein language models and protein structure models are equally good at representing features, albeit in different modalities. Therefore, we propose to quantify the sequence-structure retrieval power to reflect the alignment power of the pretrained model. Looking back at the contrastive alignment loss we used in pretraining, the loss actually includes the structure-to-sequence and sequence-to-structure alignment

calculations. The intermediate state score calculations can directly help evaluate the multi-modality alignment level. The retrieval alignment evaluation on CATH, trRosetta, Ts50/Ts500 and CASP14 test sets are shown in Group 2 of Table 1. Similarly, We also report residue-level and protein-level results, respectively. The protein-level pre-trained model is easier to align the sequences and structures with higher accuracy and lower KL distance, which satisfies the intuition. Overall, the pretrained structure module shows a strong alignment level implying that the proposed framework works well.

4.3. Downstream Evaluation

Computational protein design is the conceptual inverse of protein structure prediction, aiming to infer amino acid sequences given the corresponding atomic coordinates of the protein structure backbones. Figure 5 shows the proposed protein design model for our downstream evaluation, which directly transfers the pretrained structure model as the backbone, followed by a non-autoregressive decoder with linear MLPs. The CATH training set is used to train the protein design framework and finetune the structure model. And the CATH testing set and Ts50/Ts500 are used to score the primary results.

As shown in the Table 2, we have selected several most typical baselines of different types. Among the methods with advanced performance, ProteinMPNN [7] and GVP-transformer [16] are particularly prominent, which have more advantages in sequence recovery and model perplexity. The lightweight GVP-GNN [20] is still competitive, which is reflected in its relatively good performance and speed.

Compared to the baselines, our protein design models perform better on both perplexity and recovery metrics. It is worth mentioning that the non-autoregressive decoder in our module brings faster sampling speed.

In terms of different levels (Design_p vs. Design_r), there is no significant difference in the residue-level and protein-level pretrained modules in downstream tasks, although Design_r slightly exceeds Design_p overall. This may be due to the fact that the small gap between the two levels of pretrained models is further narrowed during the fine-tuning process.

In addition, within Group 2, we use the pretrained model and the non-trained model as the backbone for comparison. It can be found that the pretrained model significantly improves the performance in terms of perplexity and recovery, which further shows that the pretrained structure model has a stronger generalization ability in downstream tasks.

5. Conclusion

In this work, we first propose the use of pretrained protein language models to train protein structure models,

which exploit sufficient prior knowledge from robust protein language models. Furthermore, we use self-supervised contact map prediction as an auxiliary structural constraint. A series of internal tasks (e.g., contact map prediction and retrieval alignment evaluation), and external tasks (e.g., protein design) are proposed to evaluate the performance. The quantitative experimental analysis demonstrates the superiority of our pretrained framework. Although large-scale language models do help to learn effective structural information from language knowledge, related exploration is still in its infancy. In future work, we will adopt more powerful structural architecture and training constraints for the sequence-structure translation.

Appendix

Full CASP14 Targets

The full CASP14 target list we used in this work is:

T1024, T1025, T1026, T1027, T1029, T1030, T1031, T1032, T1033, T1035, T1036s1, T1037, T1038, T1039, T1040, T1041, T1042, T1043, T1044, T1046s1, T1046s2, T1049, T1050, T1054, T1056, T1064, T1067, T1073, T1074, T1079, T1080, T1082, T1090, T1099.

These are all publicly available CASP14 targets totaling 34, and we have filtered the data for which no PDB files are available.

References

- [1] Ethan C. Alley, Grigory Khimulya, Surojit Biswas, Mohammed AlQuraishi, and George M. Church. Unified rational protein engineering with sequence-based deep representation learning. *Nature Methods*, 2019. 3
- [2] Ehsaneddin Asgari and Mohammad R. K. Mofrad. Continuous distributed representation of biological sequences for deep proteomics and genomics. *PLOS ONE*, 2015. 3
- [3] Minkyung Baek, Frank DiMaio, Ivan Anishchenko, Justas Dauparas, Sergey Ovchinnikov, Gyu Rie Lee, Jue Wang, Qian Cong, Lisa N. Kinch, R. Dustin Schaeffer, Claudia Millán, Hahnbeom Park, Carson Adams, Caleb R. Glassman, Andy DeGiovanni, Jose Henrique Pereira, Andria V. Rodrigues, Alberdina A. van Dijk, Ana C. Ebrecht, Diederik J. Opperman, Theo Sagmeister, Christoph Buhlheller, Tea Pavkov-Keller, Manoj K. Rathinaswamy, Udit Dalwadi, Calvin K. Yip, John E. Burke, K. Christopher Garcia, Nick V. Grishin, Paul D. Adams, Randy J. Read, and David Baker. Accurate prediction of protein structures and interactions using a three-track neural network. *Science*, 2021. 3
- [4] Federico Baldassarre, David Menéndez Hurtado, Arne Elofsson, and Hossein Azizpour. Graphqa: protein model quality assessment using graph convolutional networks. *Bioinformatics*, 2020. 3
- [5] Tristan Bepler and Bonnie Berger. Learning protein sequence embeddings using information from structure. *arXiv preprint arXiv:1902.08661*, 2019. 1

- [6] Sheng Chen, Zhe Sun, Lihua Lin, Zifeng Liu, Xun Liu, Yutian Chong, Yutong Lu, Huiying Zhao, and Yuedong Yang. To improve protein sequence profile prediction through image captioning on pairwise residue distance map. *Journal of Chemical Information and Modeling*, 2020. 3
- [7] Justas Dauparas, Ivan Anishchenko, Nathaniel Bennett, Hua Bai, Robert J Ragotte, Lukas F Milles, Basile IM Wicky, Alexis Courbet, Rob J de Haas, Neville Bethel, et al. Robust deep learning–based protein sequence design using proteinmpnn. *Science*, 378(6615):49–56, 2022. 7, 8
- [8] Georgy Derevyanko, Sergei Grudinin, YOSHUA Bengio, and Guillaume Lamoureaux. Deep convolutional networks for quality assessment of protein folds. *Bioinformatics*, 2018. 3
- [9] Jacob Devlin, Ming-Wei Chang, Kenton Lee, and Kristina Toutanova. Bert: Pre-training of deep bidirectional transformers for language understanding. *arXiv preprint arXiv:1810.04805*, 2018. 1
- [10] Ahmed Elnaggar, Michael Heinzinger, Christian Dallago, Ghalia Rehawi, Wang Yu, Llion Jones, Tom Gibbs, Tamas Feher, Christoph Angerer, Martin Steinegger, Debsindhu Bhowmik, and Burkhard Rost. Prottrans: Towards cracking the language of life code through self-supervised deep learning and high performance computing. *IEEE Transactions on Pattern Analysis and Machine Intelligence*, 2021. 3
- [11] Zhangyang Gao, Cheng Tan, Stan Li, et al. Alphadesign: A graph protein design method and benchmark on alphafolddb. *arXiv preprint arXiv:2202.01079*, 2022. 7
- [12] Vladimir Gligorijević, P. Douglas Renfrew, Tomasz Kosciolk, Julia Koehler Leman, Daniel Berenberg, Tommi Vatanen, Chris Chandler, Bryn C. Taylor, Ian M. Fisk, Hera Vlammakis, Ramnik J. Xavier, Rob Knight, Kyunghyun Cho, and Richard Bonneau. Structure-based protein function prediction using graph convolutional networks. *bioRxiv*, 2020. 3
- [13] Yuzhi Guo, Jiayang Wu, Hehuan Ma, and Junzhou Huang. Self-supervised pre-training for protein embeddings using tertiary structures. 2022. 3
- [14] Michael Heinzinger, Ahmed Elnaggar, Yu Wang, Christian Dallago, Dmitrii Nechaev, Florian Matthes, and Burkhard Rost. Modeling the language of life – deep learning protein sequences. *bioRxiv*, 2019. 3
- [15] Pedro Hermosilla, Marco Schäfer, Matěj Lang, Gloria Fackelmann, Pere-Pau Vázquez, Barbora Kozlíková, Michael Krone, Tobias Ritschel, and Timo Ropinski. Intrinsic-extrinsic convolution and pooling for learning on 3d protein structures. *Learning*, 2020. 3
- [16] Chloe Hsu, Robert Verkuil, Jason Liu, Zeming Lin, Brian Hie, Tom Sercu, Adam Lerer, and Alexander Rives. Learning inverse folding from millions of predicted structures. *bioRxiv*, 2022. 1, 3, 4, 7, 8
- [17] Bozhen Hu, Jun Xia, Jiangbin Zheng, Cheng Tan, Yufei Huang, Yongjie Xu, and Stan Z. Li. Protein language models and structure prediction: Connection and progression. 2022. 3
- [18] Yufei Huang, Lirong Wu, Haitao Lin, Jiangbin Zheng, Ge Wang, and Stan Z Li. Data-efficient protein 3d geometric pretraining via refinement of diffused protein structure decoy. *arXiv preprint arXiv:2302.10888*, 2023. 3
- [19] John Ingraham, Vikas Garg, Regina Barzilay, and Tommi Jaakkola. Generative models for graph-based protein design. *Advances in neural information processing systems*, 32, 2019. 6, 7
- [20] Bowen Jing, Stephan Eismann, Patricia Suriana, Raphael JL Townshend, and Ron Dror. Learning from protein structure with geometric vector perceptrons. *arXiv preprint arXiv:2009.01411*, 2020. 3, 7, 8
- [21] Bowen Jing, Stephan Eismann, Patricia Suriana, Raphael J. L. Townshend, and Ron O. Dror. Learning from protein structure with geometric vector perceptrons. *Learning*, 2020. 3
- [22] John Jumper, Richard Evans, Alexander Pritzel, Tim Green, Michael Figurnov, Olaf Ronneberger, Kathryn Tunyasuvunakool, Russ Bates, Augustin Žídek, Anna Potapenko, et al. Highly accurate protein structure prediction with alphafold. *Nature*, 596(7873):583–589, 2021. 1, 6
- [23] John M. Jumper, Richard O. Evans, Alexander Pritzel, Tim Green, Michael Figurnov, Olaf Ronneberger, Kathryn Tunyasuvunakool, Russell Bates, Augustin Žídek, Anna Potapenko, Alex Bridgland, Clemens Meyer, Simon A. A. Kohl, Andrew J. Ballard, Andrew Cowie, Bernardino Romera-Paredes, Stanislav Nikolov, R. D. Jain, Jonas Adler, Trevor Back, Stig Petersen, David Reiman, Ellen Clancy, Michal Zielinski, Martin Steinegger, Michalina Pacholska, Tamas Berghammer, Sebastian Bodenstern, David L. Silver, Oriol Vinyals, Andrew W. Senior, Koray Kavukcuoglu, Pushmeet Kohli, and Demis Hassabis. Highly accurate protein structure prediction with alphafold. *Nature*, 2021. 3
- [24] Zhixiu Li, Yuedong Yang, Eshel Faraggi, Jian Zhan, and Yaoqi Zhou. Direct prediction of profiles of sequences compatible with a protein structure by neural networks with fragment-based local and energy-based nonlocal profiles. *Proteins: Structure, Function, and Bioinformatics*, 82(10):2565–2573, 2014. 6, 7
- [25] Zeming Lin, Halil Akin, Roshan Rao, Brian Hie, Zhongkai Zhu, Wenting Lu, Allan Dos Santos Costa, Maryam Fazel-Zarandi, Tom Sercu, Sal Candido, and Alexander Rives. Language models of protein sequences at the scale of evolution enable accurate structure prediction. 2022. 3
- [26] Zeming Lin, Halil Akin, Roshan Rao, Brian Hie, Zhongkai Zhu, Wenting Lu, Allan dos Santos Costa, Maryam Fazel-Zarandi, Tom Sercu, Sal Candido, et al. Language models of protein sequences at the scale of evolution enable accurate structure prediction. *bioRxiv*, 2022. 1, 3
- [27] Yuecong Min, Aiming Hao, Xiujuan Chai, and Xilin Chen. Visual alignment constraint for continuous sign language recognition. In *Proceedings of the IEEE/CVF International Conference on Computer Vision*, pages 11542–11551, 2021. 4
- [28] James O’Connell, Zhixiu Li, Jack Hanson, Rhys Heffernan, James Lyons, Kuldip Paliwal, Abdollah Dehzangi, Yuedong Yang, and Yaoqi Zhou. Spin2: Predicting sequence profiles from protein structures using deep neural networks. *Proteins: Structure, Function, and Bioinformatics*, 86(6):629–633, 2018. 7
- [29] Alec Radford, Jong Wook Kim, Chris Hallacy, Aditya Ramesh, Gabriel Goh, Sandhini Agarwal, Girish Sastry,

- Amanda Askeel, Pamela Mishkin, Jack Clark, et al. Learning transferable visual models from natural language supervision. In *International Conference on Machine Learning*, pages 8748–8763. PMLR, 2021. 2, 4
- [30] Aditya Ramesh, Prafulla Dhariwal, Alex Nichol, Casey Chu, and Mark Chen. Hierarchical text-conditional image generation with clip latents. *arXiv preprint arXiv:2204.06125*, 2022. 2
- [31] Roshan Rao, Nicholas Bhattacharya, Neil Thomas, Yan Duan, Xi Chen, John Canny, Pieter Abbeel, and Yun S. Song. Evaluating protein transfer learning with tape. *bioRxiv*, 2019. 3
- [32] Roshan Rao, Joshua Meier, Tom Sercu, Sergey Ovchinnikov, and Alexander Rives. Transformer protein language models are unsupervised structure learners. *Biorxiv*, 2020. 1, 3, 5
- [33] Roshan M Rao, Jason Liu, Robert Verkuil, Joshua Meier, John Canny, Pieter Abbeel, Tom Sercu, and Alexander Rives. Msa transformer. In *International Conference on Machine Learning*, pages 8844–8856. PMLR, 2021. 1
- [34] Alexander Rives, Siddharth Goyal, Joshua Meier, Demi Guo, Myle Ott, C. Lawrence Zitnick, Jerry Ma, and Rob Fergus. Biological structure and function emerge from scaling unsupervised learning to 250 million protein sequences. *Proceedings of the National Academy of Sciences of the United States of America*, 2019. 3
- [35] Alexander Rives, Joshua Meier, Tom Sercu, Siddharth Goyal, Zeming Lin, Jason Liu, Demi Guo, Myle Ott, C Lawrence Zitnick, Jerry Ma, et al. Biological structure and function emerge from scaling unsupervised learning to 250 million protein sequences. *Proceedings of the National Academy of Sciences*, 118(15):e2016239118, 2021. 1
- [36] Nils Strodthoff, Patrick Wagner, Markus Wenzel, and Wojciech Samek. UDSMProt: universal deep sequence models for protein classification. *Bioinformatics*, 36(8):2401–2409, 01 2020. 3
- [37] Cheng Tan, Zhangyang Gao, Jun Xia, and Stan Z Li. Generative de novo protein design with global context. *arXiv preprint arXiv:2204.10673*, 2022. 7
- [38] Yiqi Tong, Jiangbin Zheng, Hongkang Zhu, Yidong Chen, and Xiaodong Shi. A document-level neural machine translation model with dynamic caching guided by theme-rheme information. In *Proceedings of the 28th International Conference on Computational Linguistics*, pages 4385–4395, 2020. 1
- [39] Kathryn Tunyasuvunakool, Jonas Adler, Zachary Wu, Tim Green, Michal Zielinski, Augustin Žídek, Alex Bridgland, Andrew Cowie, Clemens Meyer, Agata Laydon, Sameer Velankar, Gerard J. Kleywegt, Alex Bateman, Richard Evans, Alexander Pritzel, Michael Figurnov, Olaf Ronneberger, Russell Bates, Simon A. A. Kohl, Anna Potapenko, Andrew J. Ballard, Bernardino Romera-Paredes, Stanislav Nikolov, R. D. Jain, Ellen Clancy, David Reiman, Stig Petersen, Andrew W. Senior, Koray Kavukcuoglu, Ewan Birney, Pushmeet Kohli, John M. Jumper, and Demis Hassabis. Highly accurate protein structure prediction for the human proteome. *Nature*, 2021. 3
- [40] Ashish Vaswani, Noam Shazeer, Niki Parmar, Jakob Uszkoreit, Llion Jones, Aidan N Gomez, Łukasz Kaiser, and Illia Polosukhin. Attention is all you need. *Advances in neural information processing systems*, 30, 2017. 4
- [41] Chong Wu, Jiangbin Zheng, Zhenan Feng, Houwang Zhang, Le Zhang, Jiawang Cao, and Hong Yan. Fuzzy slic: Fuzzy simple linear iterative clustering. *IEEE Transactions on Circuits and Systems for Video Technology*, 31(6):2114–2124, 2020. 1
- [42] Zachary Wu, Kadina E Johnston, Frances H. Arnold, and Kevin K. Yang. Protein sequence design with deep generative models. *arXiv: Quantitative Methods*, 2021. 3
- [43] Zuobai Zhang, Minghao Xu, Arian Jamasb, Vijil Chenthamarakshan, Aurelie Lozano, Payel Das, and Jian Tang. Protein representation learning by geometric structure pre-training. 2022. 3
- [44] Jiangbin Zheng, Yidong Chen, Chong Wu, Xiaodong Shi, and Suhail Muhammad Kamal. Enhancing neural sign language translation by highlighting the facial expression information. *Neurocomputing*, 464:462–472, 2021. 1
- [45] Jiangbin Zheng, Yile Wang, Cheng Tan, Siyuan Li, Ge Wang, Jun Xia, Yidong Chen, and Stan Z Li. Cvt-slr: Contrastive visual-textual transformation for sign language recognition with variational alignment. *arXiv preprint arXiv:2303.05725*, 2023. 4
- [46] Jiangbin Zheng, Yile Wang, Ge Wang, Jun Xia, Yufei Huang, Guojiang Zhao, Yue Zhang, and Stan Z Li. Using context-to-vector with graph retrofitting to improve word embeddings. *arXiv preprint arXiv:2210.16848*, 2022. 4